Quinalizarin as a potent, selective and cell permeable inhibitor of protein kinase CK2

Giorgio Cozza, Marco Mazzorana, Elena Papinutto, Jenny Bain, Matthew Elliott, Giovanni Di Maira, Alessandra Gianoncelli, Mario A. Pagano, Stefania Sarno, Maria Ruzzene, et al.

QUINALIZARIN AS A POTENT, SELECTIVE AND CELL PERMEABLE INHIBITOR OF PROTEIN KINASE CK2.

Giorgio COZZA[*], Marco MAZZORANA[*†], Elena PAPINUTTO[†], Jenny BAIN [§], Matthew ELLIOTT[§], Giovanni DI MAIRA[*†], Alessandra GIANONCELLI[*], Mario A. PAGANO[*†], Stefania SARNO[*†], Maria RUZZENE[*†], Roberto BATTISTUTTA[‡†], Flavio MEGGIO[*], Stefano MORO[¶], Giuseppe ZAGOTTO[¶], Lorenzo A. PINNA[*†1],

[*]Department of Biological Chemistry and CNR Institute of Neurosciences, University of Padova, viale G. Colombo 3, 35121 Padova, Italy.
[†]Venetian Institute for Molecular Medicine (VIMM), via Orus 2, 35129 Padova, Italy
[‡]Department of Chemical Sciences, University of Padova, via Marzolo 1, 35131 Padova, Italy
[¶]Molecular Modeling Section (MMS), Department of Pharmaceutical Sciences, via Marzolo 5, 35131 Padova, Italy
[§]Division of Signal Transduction Therapy and Medical Research Council, Protein Phosphorylation Unit, University of Dundee, Dundee DD1 5EH, U.K.

Running title: CK2 inhibition by quinalizarin

Abbreviations: CK2, casein kinase 2; TBB, 4,5,6,7-tetrabromo-1*H*-benzotriazole; TBI, 4,5,6,7-tetrabromo-1*H*-benzimidazole; DMAT, 2-dimethylamino-4,5,6,7-tetrabromo-1*H*-benzimidazole; TBCA, 4,5,6,7-tetrabromo-cinnamic acid; HIPK2, homeodomain-interacting protein kinase-2; PIM, provirus integration site for Moloney murine leukaemia virus; DYRK, dual-specificity tyrosine-phosphorylated and –regulated kinase; ERK, extracellular-signal-regulated kinase; PKD, protein kinase D.

[1] Correspondence: Dipartimento di Chimica Biologica, viale G. Colombo 3, 35131 Padova, Italy. Tel.: +39 049 8276108; Fax: +39 049 8073310; e-mail: lorenzo.pinna@unipd.it.

Synopsis

Emodin (1,3,8-trihydroxy-6-methyl-anthraquinone) is a moderately potent and poorly selective inhibitor of CK2, one of the most pleiotropic Ser/Thr protein kinases, implicated in neoplasia and in other global diseases. By virtual screening of the MMS database we have now identified quinalizarin (1,2,5,8-tetrahydroxy-anthraquinone) as an inhibitor of CK2 more potent and selective than emodin. CK2 inhibition by quinalizarin is competitive with respect to ATP, with a K_i value around 50 nM. Tested at 1 μM concentration on a panel of 75 protein kinases, quinalizarin drastically inhibits only CK2, with a promiscuity score (11.1) which is the lowest ever reported so far for a CK2 inhibitor. Especially remarkable is the ability of quinalizarin to discriminate between CK2 and a number of kinases, notably DYRK1a, PIMs 1, 2 and 3, HIPK2, MNK1, ERK8 and PKD1, which conversely tend to be inhibited as drastically as CK2 by commercially available CK2 inhibitors. The determination of the crystal structure of a complex between quinalizarin and CK2α subunit highlights the relevance of polar interactions in stabilizing the binding, an unusual characteristic for a CK2 inhibitor, and disclose other structural features which may account for the narrow selectivity of this compound. Tested on Jurkat cells, quinalizarin proved able to inhibit endogenous CK2 and to induce apoptosis more efficiently than the commonly used CK2 inhibitors TBB and DMAT.

Key words: apoptosis; CK2 inhibitors; drug design; HIPK2; PIM-1; quinalizarin; selectivity;

Introduction

CK2, an acronym derived from the old misnomer "casein kinase 2", denotes one of the most pleiotropic Ser/Thr protein kinases with hundreds of substrates already known many of which are implicated in fundamental cellular processes, such as gene expression, protein synthesis, proliferation, apoptosis and differentiation/transformation [reviewed by 1-4]. The CK2 holoenzyme is composed of two catalytic subunits (α and/or α') and a dimer of two non-catalytic subunits (β) that are very tightly assembled together [5]. In contrast to the majority of other protein kinases, the catalytic subunit of CK2 has never been found in an inactive conformation due to unique intramolecular constraints [6], a feature which is commonly referred to by saying that CK2 is "constitutively active". Such a lack of evident down-regulatory devices is likely to reflect the pleiotropy of this enzyme [7] but is also probably responsible for the pathogenic potential of this kinase, whose aberrantly high activity has been associated with numerous diseases [8].
Not surprisingly therefore considerable efforts have been made in recent times to develop specific cell permeable CK2 inhibitors. Several ATP site-directed CK2 inhibitors have been described to date, belonging to different chemical classes [9-13]. Some of these are effective in vitro in the pico-molar range [12], but no information is available about their selectivity for CK2. On the other hand selectivity is expected to be high in the case of a recently developed non competitive inhibitor [14] whose cell permeability however could not be demonstrated so far. Consequently for the time being the most widely used cell permeable CK2 inhibitors, with K_i values in the nano-molar range, are commercially available compounds belonging to the class of halogenated benzimidazole/triazole, notably TBB, TBI (TBBz) and DMAT. Recently, however, the selectivity of these compounds for CK2 has been shown to be not as narrow as it was believed before. The inclusion of additional members of the kinome into the panel of kinase used for selectivity profiles revealed that some enzymes, notably DYRK1a, DYRK3, PIMs 1, 2 and 3, HIPK2, ERK8 and PKD, tend to be inhibited as drastically as CK2 by one or another of these inhibitors [15]. This study also showed that within a library of more than 50 TBB and DMAT derived compounds the efficacy toward CK2 was paralleled by similar ability to inhibit also PIM1 and/or HIPK2.
This prompted us to adopt a different strategy for the identification of specific CK2 inhibitors, consisting of computer-aided virtual screening of the MMS database based on the crystal structure of the human CK2α subunit (1JWH). This scrutiny ended up with the identification of quinalizarin (1,2,5,8-tetrahydroxy-anthraquinone) as a potential CK2 inhibitor. Quinalizarin belongs to the same chemical class of compounds also comprising emodin (1,3.8-trihydroxy-6-methyl-anthraquinone) previously described as a rather promiscuous inhibitor of several protein kinases, including CK2 [16-19]. Here we show that indeed the selectivity of quinalizarin toward CK2 is superior to that of any other CK2 inhibitor tested so far, and we analyze the structural features and the functional consequences of quinalizarin binding to CK2.

EXPERIMENTAL

Inhibitors

>99% analytically pure quinalizarin was provided by Produits Chimiques ACP Chemicals Inc. (Montreal, Canada). Atomic structure was further confirmed by solving its complex with CK2α (code 3FL5). Identical biochemical and structural data were obtained with another stock of quinalizarin previously purchased by EGA-Chemie (Steinheim, Germany). Emodin, has been purchased from Sigma-Aldrich (St. Louis, USA). TBCA was synthesized as previously described [20]. TBB and benzimidazole derivatives were kindly provided by Prof. Z. Kazimierczuk (Warsaw, Poland).

Source and purification of protein kinases

Native CK2 (nCK2) was purified from rat liver [21]. Human recombinant α and β subunits of CK2 were expressed in E. coli and the holoenzyme was reconstituted and purified as previously described [22]. Single and double mutants of CK2α subunit were generated as reported in [19, 9]. The source of all the other protein kinases used for specificity assays is as previously either described or referenced [23].

Phosphorylation assays

CK2 activity was tested in a final volume of 25 µl containing 50 mM Tris-HCl pH 7.5, 100 mM NaCl, 12 mM $MgCl_2$, 100 µM synthetic peptide substrate RRRADDSDDDDD and 0.02 mM [γ-^{33}P-ATP] (500-1000 cpm/pmole), unless otherwise indicated, and incubated for 10 minutes at 37 ºC. Native CK2 purified from rat liver (0.5-1 pmol) was usually the phosphorylating enzyme, unless otherwise indicated. Assays were stopped by addition of 5 µl of 0.5 M orthophosphoric acid before spotting aliquots onto phosphocellulose filters. Filters were washed in 75 mM phosphoric acid (5-10 ml/each) four times then once in methanol and dried before counting. PIM1 activity was determined by following the same procedure by incubating the kinase in the presence of 50 mM Tris-HCl pH 7.5, 0.1% (v/v) 2-mercaptoethanol, 0.1 mM EGTA, 30 µM synthetic peptide substrate RKRRQTSMTD and 100 µM [γ-^{33}P-ATP]. HIPK2 activity was determined under the same conditions used for PIM1 assays except for ATP which was 20 µM and the use of MBP (10 µg) as phosphorylatable substrate. Conditions for the activity assays of all other protein kinases tested in selectivity experiments are described or referenced elsewhere [23].

Kinetic determination

Initial velocities were determined at each of the substrate concentration tested. K_M values were calculated either in the absence or in the presence of increasing concentrations of inhibitor, from Lineweaver-Burk double-reciprocal plots of the data. Inhibition constants were then calculated by linear regression analysis of K_M/V_{max} versus inhibitor concentration plots. Alternatively inhibition constants were also deduced from the IC_{50}/K_i Cheng-Prusoff relationship [24]. The rationale underlying this approach, based on the assumption that inhibition is competitive with respect to ATP, is illustrated by Burlingham and Widlanski [25].

Cell culturing, transfection and treatment

The human leukemia Jurkat T-cell line was maintained in RPMI-1640, while HEK-293T cells were cultured in Dulbecco's modified Eagle's medium; both mediums were supplemented with 10% (v/v) foetal calf serum, 2 mM L-glutamine, 100 units/ml penicillin and 100 µg/ml streptomycin. For transfection, HEK-293T cells were plated onto 60-mm-diameter dishes at about 80% confluency, and transiently transfected with 4 µg of Akt cDNA by standard calcium-phosphate procedure, as elsewhere described [26]. For the treatment, cells were cultured in a medium containing 1% (v/v) foetal calf serum, then incubated at 37 °C, in the presence of the compounds at the indicated concentrations. Control cells were treated with equal amounts of solvent (0.5 % v/v DMSO). For the determination of CK2 activity, at the end of incubations, cells were lysed by the addition of hypo-osmotic buffer, and 1-2 µg of cell proteins were incubated with the CK2 specific peptide in the presence of a phosphorylation mixture, as previously described [27]; alternatively, 10 µg of cell proteins were analysed by western blot with phospho-specific antibodies towards the CK2-dependent site Akt Ser129 [26]. Cell viability was assessed by means of 3-(4,5-dimethylthiazol-2-yl)-3,5-diphenyltriazolium bromide (MTT) reagent, while apoptosis/necrosis were evaluated by means of the Cell Detection Elisa kit (Roche), based on the quantification of nucleosomes present in the cytosol of the apoptotic cells or released from necrotic cells, following the manufacturer instructions. 10000 cells were used for each determination.

Crystal preparation and data collection.

The recombinant CK2 α-subunit from *Zea mays* was expressed in *Escherichia coli*, isolated and purified according to a previously described method [28]. Crystals of the CK2 complex with the inhibitor quinalizarin were obtained by co-crystallization with the sitting drop vapour-diffusion technique. A 8 mg/ml protein stock (in 25 mM Tris-Cl, 500 mM NaCl, 7 mM 2-mercaptoethanol, pH=8.5) was mixed with two volumes of a solution containing a 6-fold molar excess inhibitor in approx 2% DMSO. The mixture was incubated in ice for two hours before setting up the crystallization drops. Crystallization was performed by mixing 3 µl of the protein-inhibitor solution with 1 µl of precipitant solution (20% PEG 4000, 200 mM Na-acetate, 100 mM Na-HEPES pH=7.5) and equilibrated against a 500 µl reservoir containing the same precipitant. Trays were allowed to stand at 293 K and crystal grew in two days.
X-ray diffraction data were collected at ESRF beamline ID14 in Grenoble, at a temperature of 100 K. Crystals were cryo-protected by immersion oil type B (Hampton research). Data were indexed with MOSFLM v.6.2.6 [29] and then scaled with SCALA [30] from the CCP4 software package [31].

Structure determination and refinement.
The CK2-quinalizarin complex crystallizes in space group C2, with one molecule in the asymmetric unit. To find the best position inside the unit cell an initial rigid body transformation on the model of the apo-enzyme was adequate, using the rigid body refinement option of REFMAC 5 [CCP4 suite] [32]. The refinement was carried out using REFMAC5. Data collection and final model statistics are reported in Table 1. The presence of the inhibitors in the active site was clear since the beginning of the refinement in both Fo-Fc and 2Fo-Fc maps. The definition files for the inhibitor were created using the monomer library sketcher routine of CCP4. Refinement was carried out alternating automated cycles and manual inspection steps using the graphic program Coot v.0.5 [33]. The stereochemistry and geometric properties of the final model were checked using Coot validate analysis and Sfcheck [34] and Procheck [35] in CCP4 suite and resulted adequate for the resolution.

Data Deposition.
The coordinates for the model of CK2 in complex with quinalizarin has been deposited at the RCSB Protein Data Bank with ID code 3FL5.

Molecular modelling
For the computer aided virtual screening and molecular docking stages human CK2α subunit and PIM1 catalytic subunit were retrieved from the PDB (PDB code: 1JWH and 3BGZ, respectively). These crystal structures have shown to be the best choice to reproduce the correct pose of known crystallized inhibitors, during the protocol calibration phase (data not shown). Both structures were considered with a constitutive water molecule [36], while all the other ligands and cofactors were removed; in the case of 1JWH the CK2 conserved water molecule was added to the crystal structure. Hydrogen atoms were added to the protein structure using standard geometries with the MOE program [37]. To minimize contacts between hydrogens, the structures were subjected to Amber94 force field minimization until the rms of conjugate gradient was <0.1 kcal mol^{-1} $Å^{-1}$ keeping the heavy atoms fixed at their crystallographic positions. To strictly validate the model generated and to calibrate the high-throughput docking protocol, a small database of known PIM1 and CK2 inhibitors was built and a set of docking runs were performed using four different algorithms (MOE-Dock, Glide, FlexX, and Gold) and four different scoring functions (Moe-score, Glide-score, FlexX-score and X-score). After the calibration phase a computer aided virtual screening using the MMS-database (more than 3000 both synthetic and natural compounds) and a semiflexible ligand-docking steps were performed essentially as previously described [38, 39].
A detailed description of the molecular docking protocol together with analytical data is shown in Supplementary Material.

RESULTS

Emodin (1,3,8-trihydroxy-6-methyl-anthraquinone) the active principle of herbal medicine extracted from *Rheum palmatum*, originally reported in the literature as a fairly specific inhibitor of some tyrosine kinases [16, 17], was later found to inhibit the Ser/Thr kinase CK2 even more effectively [18]. In contrast several other non substituted hydroxyanthraquinones differing from emodin in the number and position of hydroxy groups, notably chrysophanic acid, aloe emodin and 1,8-dihydroxy-anthraquinone, display negligible inhibitory efficacy toward CK2 [40] (see also Fig. 1A). However in a computer aided virtual screening of the MMS-database, based on the crystal structure of human CK2 (1JWH), quinalizarin (1,2,5,8-tetrahydroxy-anthraquinone, see Fig. 1A) has been found to sit in the top 10% of the ranked database independently of the nature of the used scoring function.

This prompted us to assay quinalizarin as a CK2 inhibitor, by performing the kinetic experiments illustrated in Fig. 1B. The results show that quinalizarin is indeed a powerful inhibitor of CK2, competitive with respect to ATP: its K_i value (around 60 nM) is lower than those of emodin and TBB [41] and comparable to that of TBCA [20].

Next we wanted to assess the selectivity of quinalizarin by testing its inhibitory potency on a panel of 75 protein kinases. The selectivity profile was run at 1 μM concentration, sufficient to inhibit CK2 activity more than 90%. As shown in Fig. 2 under these conditions the residual CK2 activity was about 7%. By sharp contrast, none of the other kinases was inhibited as drastically as CK2, with the second most inhibited kinase (PIM3) still exhibiting more than 50% residual activity, followed by DYRK1A, DYRK3 and PIM1, whose residual activity was 60% or more. The K_i values for the inhibition of these kinases by quinalizarin were calculated (Table 2) and found to be one to two order of magnitude higher than that of CK2, a difference sufficient to ensure a clear-cut discrimination of CK2 among other kinases susceptible to quinalizarin inhibition. By contrast some of these kinases, notably PIM1 and PIM3 were inhibited by emodin as well as by the commercially available CK2 inhibitors TBB, DMAT and TBI more drastically than by quinalizarin.

The remarkable selectivity of quinalizarin prompted us to compare it with that of TBCA, another CK2 inhibitor whose efficacy is sufficiently high to profile its selectivity at a concentration of 1 instead of 10 μM. TBCA was previously tested at 10 μM concentration on a panel of 28 PKs, disclosing its ability to discriminate between CK2 and DYRK1a [20], a kinase often affected by CK2 inhibitors. That panel however didn't include a number of kinases later shown to be inhibited by TBB, DMAT and other CK2 inhibitors as drastically as CK2 itself [15]. The new data with TBCA (1 μM) on a panel of 72 PKs are now displayed in Fig. 2, lower panel, where they are compared with those obtained with 1 μM quinalizarin (upper panel). They confirm that kinases of the DYRK family are much less susceptible to TBCA (as well as to quinalizarin) than is CK2. However they also show that kinases of the PIM family tend to be inhibited more drastically by TBCA than they are by quinalizarin and that two other kinases either unaffected or poorly affected by quinalizarin, MNK1 and ERK8, are inhibited 75% or more by 1 μM TBCA.

Higher selectivity toward CK2 of quinalizarin as compared to TBCA is also reflected in a lower promiscuity score, expressing the average inhibition of the PKs of the panel by an inhibitor concentration sufficient to suppress CK2 activity (residual activity <10%) [15]. As calculated in Fig. 2 the promiscuity score of quinalizarin (11.13) is below that of TBCA (15.7). It is also much lower than those calculated for the typical CK2 inhibitors TBB, TBI (TBBz) and DMAT (see [15]). In summary it appears that quinalizarin is the most selective CK2 inhibitor analyzed, with a potency, in terms of K_i value, comparable to those of the most powerful of these inhibitors, notably TBCA, DMAT, DBC and NBC [20, 10]

Somewhat surprisingly the two unique CK2 hydrophobic residues shown to play a prominent role in the interaction with the majority of CK2 inhibitors, V66 and I174, appear to be only of marginal relevance in the case of quinalizarin, whose IC_{50} value is poorly affected by their mutation to

alanine. In contrast these mutations and especially the double mutant cause a more than 50-fold increase in IC_{50} for emodin (see Fig. 3).

To get a better insight into the mode of binding of quinalizarin and try to disclose the structural basis for its selectivity, the 3D structure of a complex between quinalizarin and CK2α (from *Z. mays*) has been solved. As shown in Fig 4A, quinalizarin makes polar interactions with CK2 using at least three of its hydroxy groups: the one at position 2 is hydrogen bonded with the conserved water molecule(1) and Lys68 (which is also near to quinalizarin hydroxyl group 2, 3.3 Å from it), the one at position 5 interacts with the hinge region (carbonyl backbone of V116) through another water molecule, while the hydroxyl group 8 makes a very stable polar interaction with H160 and the backbone carbonyl group of R47. This latter occurs through hydrogen bonds among the three atoms at almost the same distance, giving rise to a sort of equilateral triangle and stabilizing the kinase into a close conformation which entraps the inhibitor inside the pocket (Fig. 5). Note in this respect that although the scaffold of quinalizarin in this structure is coplanar and super-imposable to that of emodin in its complex with human CK2 (3BQC, see fig.4B) [42] the lack of a hydroxyl group in position 5 in emodin prevents the formation of the interaction with H160 and the backbone of R47 found with quinalizarin.

Since crystallographic data are not yet available for PIM1 kinase in complex with quinalizarin or emodin, a molecular docking of these inhibitors with PIM1 was performed (Fig. 6). This discloses structural features accounting, on the one hand, for the higher susceptibility of this kinase to emodin, and on the other, for its reduced sensitivity to quinalizarin. Although both inhibitors can be accommodated in the binding cleft of PIM1 in a position similar to that observed in the two crystal structures of CK2 discussed above (3BQC and 3FL5 for emodin and quinalizarin, respectively), they have to face at least three important amino acid substitutions. Firstly, the replacement in PIM1 of the CK2 water-exposed Y50 with F49 (PIM3 carries the same substitution), which is oriented inside the cleft, puts both inhibitors in contact with this hydrophobic side chain; while emodin can take advantage of this apolar interaction due to its more hydrophobic characteristics, F49 will negatively affect quinalizarin binding, mainly for an unfavourable interaction with OH^8, at only 3.6 Å from the Phe aromatic side chain. Note that in the corresponding position (5), emodin does not carry any functional group.

Secondly, PIM1 replaces CK2 M163 with L174. Also in this case the docking mechanism suggests an unfavourable interaction between the OH^5 and L174, at only 3.5 Å. In this situation the OH^5 cannot make an interaction with a water molecule as in the case of CK2. On the other hand, emodin is attracted towards L174, preserving the interaction between OH^3 and the conserved water molecule, but making a rotation of about 30 degrees with respect to the quinalizarin position. This places emodin in a more favourable hydrophobic subsite, formed by L44, V126 and L174. At the same time with this new interaction the OH^8 of emodin is hydrogen-bonded to the backbone carbonyl group of E121, at 2.7 Å distance. Finally due to the substitution of H160 with E171, PIM1 is not able to make the same interaction of quinalizarin OH^8 observable in the crystal structure of its complex with CK2.

It is interesting to note that only 21% of the protein kinases included in the selectivity panel have a tyrosine residue at the position homologous to CK2 Y50 and only 10% have a methionine homologous to CK2 M163. Almost all the kinases belonging to this latter group have a phenylalanine instead of tyrosine-50. Moreover inside the selectivity panel CK2 is the only kinase bearing the H160 residue. It can be concluded therefore that CK2 possesses a particular combination of residues that could explain the remarkable selectivity of quinalizarin.

In order to see if quinalizarin is cell permeable, advantage has been taken of two cell lines: HEK293T cells which can be easily transfected with Akt whose phosphorylation by CK2 at Ser129 can be specifically monitored by anti pS129 antibodies [26] and Jurkat cells which have been commonly used in the past to measure the cytotoxic and pro-apoptotic efficacy of many CK2 inhibitors. Treatment of HEK293T cells with 5 μM quinalizarin (Fig. 7A) is sufficient to reduce Akt S129 phosphorylation by >60%, i.e. more efficiently than treatment with 25 μM TBB. Similar

results were obtained with Jurkat cells whose 4 hr treatment with 5 μM quinalizarin is sufficient to induce a 48 ± 5% drop of CK2 activity in the cell lysates, whereas the efficacy of TBB is hardly detectable at this concentration (11 + 6% inhibition). Consistent with this quinalizarin is also more effective than TBB in inducing cell death (Fig. 7B). Interestingly cell death induced by quinalizarin is mainly accounted for by apoptosis with just a minor contribution from necrosis (Fig. 7C). Necrosis is instead more accentuated in the case of TBB and, even more, of DMAT, where it predominates over apoptosis. Since we know that several other kinases (especially those of the DYRK, HIPK and PIM families) are drastically inhibited by DMAT, and to a lesser extent by TBB [15] it is tempting to ascribe the necrosis observed with these CK2 inhibitors to the targeting of protein kinases other than CK2.

DISCUSSION

For the time being and to the best of our knowledge quinalizarin is the most selective CK2 inhibitor with K_i in the low nanomolar range whose specificity has been profiled on large panels of protein kinases (70 or more). This reflects in a particularly low "promiscuity score", expressing the average inhibition of all the kinases of the panel, measured at a concentration of the inhibitor sufficient to inhibit activity drastically (>90%), but not to fully suppress the activity of the kinase of interest [15]. This value in the case of quinalizarin drops to 11.1, below that of TBCA (15.7) (see Fig. 2), not to mention TBB (47.3), TBI/TBBz (53), DMAT (49.31) and even the improved DMAT derivative K66 (19.3) [15].

Especially noteworthy is the observation that by testing quinalizarin at a concentration of 1 μM on a panel of 75 kinases CK2 is inhibited by 93 %, with the second most inhibited kinase (PIM3) being still >50% active and displaying a IC_{50} value (1.73 μM) >15-fold higher than that of CK2 (0.11 μM). These data are particularly striking if it is born in mind that quinalizarin is structurally very similar to emodin, a quite promiscuous inhibitor of CK2 and of several other protein kinases as well, whose potency toward PIM3 (IC_{50}= 0.08 μM) is 30-fold higher than that toward CK2 (IC_{50} = 2.50 μM)

The determination of the crystal structure of a complex between quinalizarin and CK2, in conjunction with the availability of the structure of PIM1 (whose behaviour with emodin as opposed to quinalizarin is similar to that of PIM3) has disclosed a number of structural features that may account for the marked predilection of quinalizarin for CK2. Of crucial relevance appears to be the presence in quinalizarin of the hydroxyl group at position 8, forming with those at positions 2 and 5 a triad of hydroxyls which make possible three strong polar interactions within the active site of CK2.These take place with: i) a water molecule present in all CK2 structures and with K68 nearby; ii) the backbone of the hinge region, through a second water molecule, and, iii) with the backbone of R47 and with H160 (see Fig. 4A), respectively. These interactions, moreover, force the kinase to adopt a close conformation which favours the entrapping of the inhibitor (Fig. 5). In emodin the hydroxyl groups at positions 1 and 8 are conserved but the one at position 5 is not (see Fig. 1A) and the one at position 2 is shifted to position 3. As a consequence, emodin cannot make the same triad of hydrogen bonds observed with quinalizarin: as observed in the 3BQC structure, it can make two polar interactions (i and ii, respectively) using hydroxyls 3 and 8, but not the third one (iii) with R47 and H160. An additional disadvantage of emodin is that OH^1 and the methyl group have an unfavorable environment, therefore contributing in a negative way to the energetics of binding in comparison with quinalizarin. In the 3BQC structure, the OH^1 is situated in a substantially hydrophobic environment in the deeper part of the cavity, near I66, V95, F113 and V116, while the CH_3 in position 6 is exposed to the solvent. In another available emodin/CK2 complex (1F0Q), emodin has an inverted orientation [43], but again with the methyl group in an unfavorable hydrophilic environment near K68 and E81. This can explain, at least in part, the higher potency of Q1, where these adverse interactions are absent, compared to emodin.

Although the scaffolds of emodin and quinalizarin are superimposed so that they make similar apolar contacts with a number of hydrophobic side chains, the mutation of two of these (V66 and I174) to alanine causes a 55-fold drop in inhibitory efficacy with emodin, while having an only marginal effect with quinalizarin (see Fig.3). This is not straightforward to explain based solely on the crystal structure of the wild type kinase; probably more general solvation/desolvation effects must be considered, taking into account the more hydrophobic character of emodin compared to quinalizarin as well as the possibility that the introduction of a mutation can also significantly alter the binding mode of the ligand.

In the same vein it should be noted that in PIM1 and in many other kinases: i) Y50 which in CK2 is oriented outwards owing to its hydrophilic hydroxyl, is replaced by more hydrophobic phenylalanine, which implies an orientation inside the cleft (as shown by modelling in Fig. 6); ii) M163 is replaced by L174; iii) H160 is replaced by E171. These three features favour the accommodation of emodin (with the Phe side chain pointing towards the methyl group) while hindering that of quinalizarin, forced to face the hydrophobic side chain of Phe and Leu with its hydrophilic –OH groups at positions 8 and 5. Interestingly, among all the kinases belonging to the selectivity panel, only CK2 can accomplish at the same time all the three quinalizarin binding optimizing interactions.

Similar to emodin [41], TBB [27], DMAT [44] and several other CK2 inhibitors [10] quinalizarin is also cell permeable, as judged from its ability to inhibit endogenous CK2 in HEK293 and Jurkat cells. Such an inhibition, which is higher than that observed with TBB, correlates with a marked cytotoxic efficacy (see Fig. 7B). It should be noted however that at variance with TBB and DMAT, whose cytotoxic effect is substantially (and in the case of DMAT predominantly) accounted for by necrosis, quinalizarin only marginally increases necrosis, with a much more remarkable enhancement of apoptosis (Fig. 7C). Such behaviour, reminiscent of that of etoposide, a typical apoptosis inducer, in conjunction with the narrow selectivity of quinalizarin for CK2, corroborates the notion that inhibition of CK2 mainly results in apoptosis. This raises the possibility that the necrotic effect observed with other CK2 inhibitors is at least partially due to the inhibition of protein kinases other than CK2. It may be pertinent to note in this respect that DMAT, whose necrotic effect is much more pronounced than its pro-apoptotic efficacy, is the least selective among the three inhibitors tested in Fig. 7B, with ERK8, PKD1, DYRKs 1a, 2 and 3, PIMs 1, 2, 3 and HIPK 2 and 3 inhibited as drastically or even more drastically than CK2 itself [15].

ACKNOWLEDGMENTS

We are grateful to Professor Sir Philip Cohen (MRC Protein Phosphorylation Unit, University of Dundee, Dundee, Scotland, UK) for critical reading of the manuscript. This work was supported by grants to L.A.P. from AIRC, European Commission (PRO-KINASERESEARCH 503467), and by the Italian Cystic Fibrosis Research Foundation (grant FFC#4/2007) with the contribution of “Banca Popolare di Verona e Novara” and “Fondazione Giorgio Zanotto”.

REFERENCES

1 Meggio, F. and Pinna, L.A. (2003) One-thousand-and-one substrates of protein kinase CK2? FASEB J. **17**, 349-368.
2 Pinna, L.A. (2002) Protein kinase CK2: a challenge to canons. J. Cell Sci. **115**, 3873-3878.
3 Litchfield, D.W. (2003) Protein kinase CK2: structure, regulation and role in cellular decisions of life and death. Biochem J. **369**, 1-15.
4 Ahmad, K.A., Wang, G., Unger, G., Slaton, J., Ahmed, K. (2008) Protein kinase CK2 - a key suppressor of apoptosis. Adv. Enzyme Regul. **48**, 179-187.

5 Raaf, J., Brunstein, E., Issinger, O.-G. and Niefind, K. (2008) The interaction of CK2alpha and CK2beta, the subunits of protein kinase CK2, requires CK2beta in a preformed conformation and is enthalpically driven. Protein Sci. **17**, 2180-2186.

6 Niefind, K., Yde, C.W., Ermakova, I. and Issinger O.-G. (2007) Evolved to be active: sulfate ions define substrate recognition sites of CK2alpha and emphasise its exceptional role within the CMGC family of eukaryotic protein kinases. J. Mol. Biol. **370**, 427-438.

7 Pinna, L.A. (2003) The raison d'etre of constitutively active protein kinases: the lesson of CK2. Acc. Chem. Res. **36**, 378-384.

8 Guerra, B. and Issinger, O.-G. (2008) Protein kinase CK2 in human diseases. Curr. Med. Chem. **15**, 1870-1886.

9 Pagano, M.A., Andrzejewska, M., Ruzzene, M., Sarno, S., Cesaro, L., Bain, J., Elliott, M., Meggio, F., Kazimierczuk, Z. and Pinna, LA. (2004) Optimization of protein kinase CK2 inhibitors derived from 4,5,6,7-tetrabromobenzimidazole. J. Med. Chem. **47**, 6239-6247.

10 Meggio, F., Pagano, M.A., Moro, S., Zagotto, G., Ruzzene, M., Sarno, S., Cozza, G., Bain, J., Elliott, M., Deana, A,D., Brunati, A.M., Pinna, L.A. (2004) Inhibition of protein kinase CK2 by condensed polyphenolic derivatives. An in vitro and in vivo study. Biochemistry **43**, 12931-12936.

11 Sarno, S., Salvi, M., Battistutta, R., Zanotti, G. and Pinna, L.A. (2005) Features and potentials of ATP-site directed CK2 inhibitors. Biochim. Biophys. Acta **1754**, 263-270.

12 Nie, Z., Perretta, C., Erickson, P., Margosiak, S., Almassy, R., Lu, J., Averill, A., Yager, K.M. and Chu, S. (2007) Structure-based design, synthesis, and study of pyrazolo[1,5-a][1,3,5]triazine derivatives as potent inhibitors of protein kinase CK2. Bioorg. Med. Chem. Lett. **17**, 4191-4195.

13 Nie, Z., Perretta, C., Erickson, P., Margosiak, S., Lu, J., Averill, A., Almassy, R. and Chu, S. (2008) Structure-based design and synthesis of novel macrocyclic pyrazolo[1,5-a] [1,3,5]triazine compounds as potent inhibitors of protein kinase CK2 and their anticancer activities. Bioorg. Med. Chem. Lett. **18**, 619-623.

14 Prudent, R., Moucadel, V., Laudet, B., Barette, C., Lafanechère, L., Hasenknopf, B., Li, J., Bareyt, S., Lacôte, E., Thorimbert, S., Malacria, M., Gouzerh, P. and Cochet, C. (2008) Identification of polyoxometalates as nanomolar noncompetitive inhibitors of protein kinase CK2. Chem. Biol. **15**, 683-692.

15 Pagano, M.A., Bain, J., Kazimierczuk, Z., Sarno, S., Ruzzene, M., Di Maira, G., Elliott, M., Orzeszko, A., Cozza, G., Meggio, F. and Pinna, L.A. (2008) The selectivity of inhibitors of protein kinase CK2: an update. Biochem. J. **415**, 353-365.

16 Chan, T.C., Chang, C.J., Koonchanok, N.M. and Geahlen, R.L. (1993) Selective inhibition of the growth of ras-transformed human bronchial epithelial cells by emodin, a protein-tyrosine kinase inhibitor. Biochem. Biophys. Res. Commun. **193**, 1152-1158.

17 Zhang, L., Lau, Y.K., Xi, L., Hong, R.L., Kim, D.S., Chen, C.F., Hortobagyi, G.N., Chang, C. and Hung, M.C. (1998) Tyrosine kinase inhibitors, emodin and its derivative repress HER-2/neu-induced cellular transformation and metastasis-associated properties. Oncogene **16**, 2855-63.

18 Yim, H., Lee, Y.H., Lee, C.H. and Lee, S.K. (1999) Emodin, an anthraquinone derivative isolated from the rhizomes of Rheum palmatum, selectively inhibits the activity of casein kinase II as a competitive inhibitor. Planta Med. **65**, 9-13.

19 Sarno, S., De Moliner, E., Ruzzene, M., Pagano, M.A., Battistutta, R., Bain, J., Fabbro, D., Schoepfer, J., Elliott, M., Furet, P., Meggio, F., Zanotti, G. and Pinna, L.A. (2003) Biochemical and 3D-structural data on the specific inhibition of protein kinase CK2 by ((5-oxo-5,6-dihydro-indolo(1,2-a)quinazolin-7-yl)acetic acid) (IQA). Biochem. J. **374**, 639-646.

20 Pagano, M.A., Poletto, G., Di Maira, G., Cozza, G., Ruzzene, M., Sarno, S., Bain, J., Elliott, M., Moro, S., Zagotto, G., Meggio, F. and Pinna, L.A. (2007) Tetrabromocinnamic acid

(TBCA) and related compounds represent a new class of specific protein kinase CK2 inhibitors. Chembiochem. **8**, 129-139.

21 Meggio, F., Donella Deana, A. and Pinna, L. (1981) Endogenous phosphate acceptor proteins for rat liver cytosolic casein kinases. J. Biol. Chem. **256**, 11958-11961.

22 Sarno, S., Vaglio, P., Meggio, F., Issinger, O.-G. and Pinna, L.A. (1996) Protein kinase CK2 mutants defective in substrate recognition. Purification and kinetic analysis. J. Biol. Chem. **271**, 10595-10601.

23 Bain, J., Plater, L., Elliott, M., Shpiro, N., Hastie, J., McLauchlan, H., Klevernic, I., Arthur, S., Alessi, D. and Cohen, P. (2007) The selectivity of protein kinase inhibitors; a further update. Biochem. J. **408**, 297-315.

24 Cheng, Y.-C. and Prusoff, W.H. (1973) Relationship between the inhibition constant (K1) and the concentration of inhibitor which causes 50 per cent inhibition (I50) of an enzymatic reaction. Biochem. Pharmacol. **22**, 3099-3108.

25 Burlingham, T.B. and Widlanski, T.S. (2003) An intuitive look at the relationship of K_i and IC_{50}: a more general use of the Dixon plot. J. Chem. Ed. **80**, 214-218.

26. Di Maira, G., Salvi, M., Arrigoni, G., Marin, O., Sarno, S., Brustolon, F., Pinna, L.A. and Ruzzene, M. (2005) Protein kinase CK2 phosphorylates and upregulates Akt/PKB. Cell Death Differ. **12**, 668-677.

27 Ruzzene, M., Penzo, D. and Pinna, L.A. (2002) Protein kinase CK2 inhibitor 4,5,6,7-tetrabromobenzotriazole (TBB) induces apoptosis and caspase-dependent degradation of haematopoietic lineage cell-specific protein 1 (HS1) in Jurkat cells. Biochem. J. **364**, 41-47.

28 Guerra, B., Niefind, K., Pinna, L.A., Schomburg, D. and Issinger, O.-G. (1998) Expression, purification and crystallization of the catalytic subunit of protein kinase CK2 from Zea mays. Acta Crystallogr. **D54**, 143-145.

29 Leslie, A.G.W. (1991) Crystallographic Computing V (Moras, D., Podjarny, A.D. and Thierry, J.P. eds), pp 27-38, Oxford University Press, Oxford In.

30 Evans, P.R. (1993) Data reduction. In Proceedings of CCP4 Study Weekend on Data Collection & Processing, pp. 114-122.

31 Collaborative Computational Project, Number 4 (1994) The CCP4 Suite: Programs for Protein Crystallography. Acta Cryst. **D50**, 760-763.

32 Murshudov, G.N., Vagin, A.A. and Dodson, E.J. (1997) Refinement of Macromolecular Structures by the Maximum-Likelihood Method. Acta Cryst. **D53**, 240-255.

33 Emsley, P. and Cowtan, K. (2004) Coot: model-building tools for molecular graphics. Acta Cryst. **D60**, 2126-2132.

34 Vaguine, A.A., Richelle, J. and Wodak, S.J. (1999) SFCHECK: a unified set of procedure for evaluating the quality of macromolecular structure-factor data and their agreement with atomic model. Acta Cryst. **D55**, 191-205.

35 Laskowski, R., MacArthur, M.W., Moss, D. and Thornton, J. (1993) Procheck: A program to check the stereochemical quality of protein structures. J. Appl. Cryst. **26**, 283-291.

36 Battistutta, R., Mazzorana, M., Cendron, L., Bortolato, A., Sarno, S., Kazimierczuk, Z., Zanotti, G., Moro, S. and Pinna, L.A. (2007) The ATP-binding site of protein kinase CK2 holds a positive electrostatic area and conserved water molecules. Chembiochem. **8**, 1804-1809.

37 Molecular Operating Environment (MOE 2006.03), C.C.G., Inc., 1255 University St., Suite 1600, Montreal, Quebec, Canada H3B 3X3.

38 Cozza, G., Bonvini, P., Zorzi, E., Poletto, G., Pagano, M. A., Sarno, S., Donella-Deana, A., Zagotto, G., Rosolen, A., Pinna, L.A., Meggio, F. and Moro, S. (2006) Identification of ellagic acid as potent inhibitor of protein kinase CK2: a successful example of a virtual screening application. J. Med. Chem. **49**, 2363-2366.

39 Cozza, G., Gianoncelli, A., Montopoli, M., Caparrotta, L., Venerando, A., Meggio, F., Pinna, L.A., Zagotto, G. and Moro, S. (2008) Identification of novel protein kinase CK1 delta (CK1δ) inhibitors through structure-based virtual screening. Bioorg. Med. Chem. Lett. **18**, 5672-5675.

40 Sarno, S., Moro, S., Meggio, F., Zagotto, G., Dal Ben, D., Ghisellini, P., Battistutta, R., Zanotti, G. and Pinna, L.A. (2002) Toward the rational design of protein kinase casein kinase-2 inhibitors. Pharmacol. Ther. **93**, 159-168.

41 Sarno, S., Reddy, H., Meggio, F., Ruzzene, M., Davies, S.P., Donella-Deana, A., Shugar, D. and Pinna, L.A. (2001) Selectivity of 4,5,6,7-tetrabromobenzotriazole, an ATP site-directed inhibitor of protein kinase CK2 ("casein kinase-2"). FEBS Lett. **496**, 44-48.

42 Raaf, J., Klopffleisch, K., Issinger, O.-G. and Niefind, K.(2008) The catalytic subunit of human protein kinase CK2 structurally deviates from its maize homologue in complex with the nucleotide competitive inhibitor emodin. J. Mol. Biol. 377, 1-8.

43 Battistutta, R., Sarno, S., De Moliner, E., Papinutto, E., Zanotti, G. and Pinna, L.A. (2000) The replacement of ATP by the competitive inhibitor emodin induces conformational modifications in the catalytic site of protein kinase CK2. J. Biol. Chem. **275**, 29618-29622.

44 Pagano, M.A., Meggio, F., Ruzzene, M., Andrzejewska, M., Kazimierczuk, Z. and Pinna, L.A. (2004) 2-Dimethylamino-4,5,6,7-tetrabromo-1*H*-benzimidazole: a novel powerful and selective inhibitor of protein kinase CK2. Biochem. Biophys. Res. Commun. **321**, 1040-1044.

LEGENDS TO FIGURES

Fig. 1:
A: Molecular structure of quinalizarin, of related compounds and of other CK2 inhibitors discussed in this paper. The values of IC_{50} reported for each compound are either drawn from [40] or have been determined under conditions described in the Experimental Section.
B: Competitive inhibition of CK2 by quinalizarin. CK2 activity was determined as described in the Experimental Section in the presence of the indicated concentrations of inhibitor. K_i was calculated from the K_m/V_{max} vs [i] replot shown in the inset. The data represent the means of experiments run in triplicate with SEM never exceeding 10%.

Fig. 2: Selectivity profiling of quinalizarin and TBCA
Inhibition assays were performed at 1 μM concentration of the indicated inhibitor under conditions described or referenced in the Experimental Section. On the right the values of promiscuity scores (PS) are shown, calculated as described in [15].

Fig. 3: CK2 inhibition by quinalizarin is marginally affected by Val66 and Ile174 substitutions. IC_{50} values were calculated by determining the activity of CK2, either wild type or mutants, at 20 μM ATP with increasing concentration of inhibitors, The ratio between the IC_{50} value of each mutants and the IC_{50} value of CK2 wild type was then calculated. Additional details are given in the Experimental Section.

Fig. 4: Structural insight into CK2α-quinalizarin complex. The 2D cartoon summarizes the main polar interactions observed in the crystal structures of CK2α complexed with quinalizarin (panel A) and emodin (panel B). Further details are given in the text.

Fig. 5: Close-up view of the inhibitor quinalizarin (yellow carbon atoms) bound to CK2 (in green). Note the closed conformation of the enzyme, with the interactions between R47, H160 and the quinalizarin OH (blue dotted line). For comparison, the open conformation of the Gly-rich loop and H160 (in magenta) in the emodin complex is shown. The yellow arrows indicate the movement from the open to the closed conformation.

Fig. 6: Molecular docking of quinalizarin by PIM1. The interactions of emodin (left panel) and of quinalizarin (right panel) with the most crucial amino acids of PIM1 catalytic site are highlighted. Molecular modelling is described in the Experimental Section. Further details are given in the text.

Fig. 7: Effect of cell treatment with quinalizarin.
A. HEK 293T cells were transfected with Akt and treated, where indicated, with quinalizarin (Quina, 5 μM or 20 μM Q1), or TBB (25 μM). Endogenous CK2 activity was analysed by western blot of cell lysates (10 μg of proteins) with antibodies towards the CK2 phospho-specific site Ser129 of Akt, or total Akt as a control. The results are also shown as a bar graph for phospho-Ser129 signal normalized to total Akt.
B. Jurkat cells were treated for 24 h with increasing concentrations of the indicated inhibitors. Cell viability was assessed by the MTT method, assigning 100% value to the control cells, treated with the solvent. Reported values represent the means +S.E.M. from four separate experiments.
C. Jurkat cells were treated for 4h with solvent (Contr), or quinalizarin (Quina, 5 μM), TBB (5 μM) and DMAT (25 μM), as indicated. Treatment with 25 μM etoposide (Eto) was used as a positive control. Apoptosis and necrosis were evaluated by quantification of nucleosomes in the cytosol (apoptotic cells) or in extracellular medium (released by necrotic cells) using the Cell Death Detection Elisa kit (Roche).

Table 1: Structural data of the quinalizarin-CK2α complex.

Data collection (ESRF beamline ID14, λ = 0.9340 Å)	
Space group	C2
Cell dimensions	
a, *b*, *c* (Å)	142.7, 61.1, 44.8
α, β, γ (°)	90.0, 103.0, 90.0
Total number of observations	49129 (7176)
Total number unique	15986 (2321)
Resolution (Å)	55.9 - 2.30 (2.42)
R_{sym} (%)	5.0 (15.3)
R_{meas} (%)	6.1 (18.4)
Mean I/σ(I)	17.6 (8.0)
Completeness (%)	95.4 (95.3)
Multiplicity	3.1 (3.1)
B_{wilson} (Å^2)	27.7
Solvent content (%)	49.3
Refinement (Final model PDB code = 3FL5)	
Resolution (Å)	2.30
No. of reflections (reference set)	15182 (804, 5%)
R_{crys}/R_{free}	18.3/23.5
No. atoms (Average B-values (Å^2))	
All atoms	2957 (16.4)
Protein	2715 (15.5)
Ligands: quinalizarin; PEG	20 (12.7); 7 (22.2)
Water	215 (27.5)
Root mean square deviations from ideality	
Bond lengths	0.008
Bond Angles	1.082
Ramachandran plot statistics (%) (excl. Gly, Pro)	
Most favoured regions	91.8
Additionally allowed regions	8.2
Generously allowed regions	0
Disallowed regions	0

Biochemical Journal Immediate Publication. Published on 11 May 2009 as manuscript BJ20090069

Table 2: K_i of CK2 inhibitors for selected protein kinases.

Inhibition constants of quinalizarin and emodin were determined according to the procedures described in the Experimental Section. The reported values represent the means obtained from at least three independent experiments with the SD never exceeding 15%.

Inhibitor	K_i (μM)				
	CK2	DYRK1a	PIM1	PIM3	HIPK2
quinalizarin	0.052	5.850	1.382	1.205	1.956
emodin	1.250	2.815	0.283	0.048	8.105
TBB[a]	0.049	2.906	0.690	0.320	3.096
TBI[a]	0.139	1.408	0.076	0.026	0.550
DMAT[a]	0.045	0.270	0.096	0.036	0.212

[a]Drawn from ref. [15] and calculated according to Cheng-Prusoff equation [24].

Biochemical Journal Immediate Publication. Published on 11 May 2009 as manuscript BJ20090069

Figure 1

A

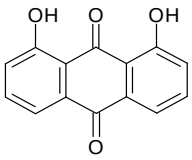

1,8-dihydroxy-anthraquinone
IC_{50} = >40 μM

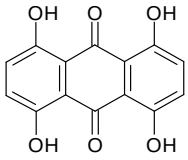

1,4,5,8-tetrahydroxy-anthraquinone
IC_{50} = >40 μM

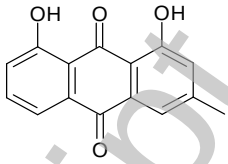

chrysophanic acid
IC_{50} = >40 μM

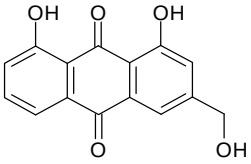

aloe emodin
IC_{50} = 28 μM

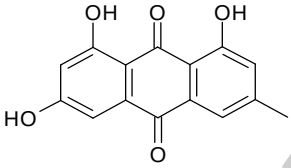

Emodin
IC_{50} = 2 μM

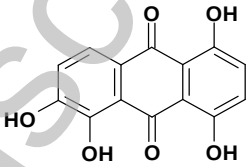

Quinalizarin
IC_{50} = 0.11 μM

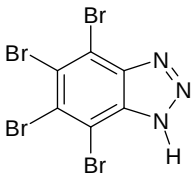

TBB
IC_{50}=0.08 μM

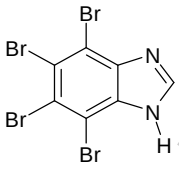

TBI
IC_{50}=0.34 μM

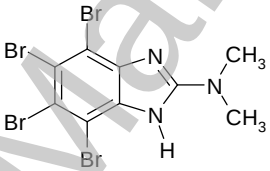

DMAT
IC_{50}=0.07 μM

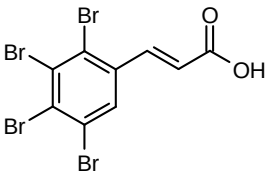

TBCA
IC_{50}=0.11 μM

B

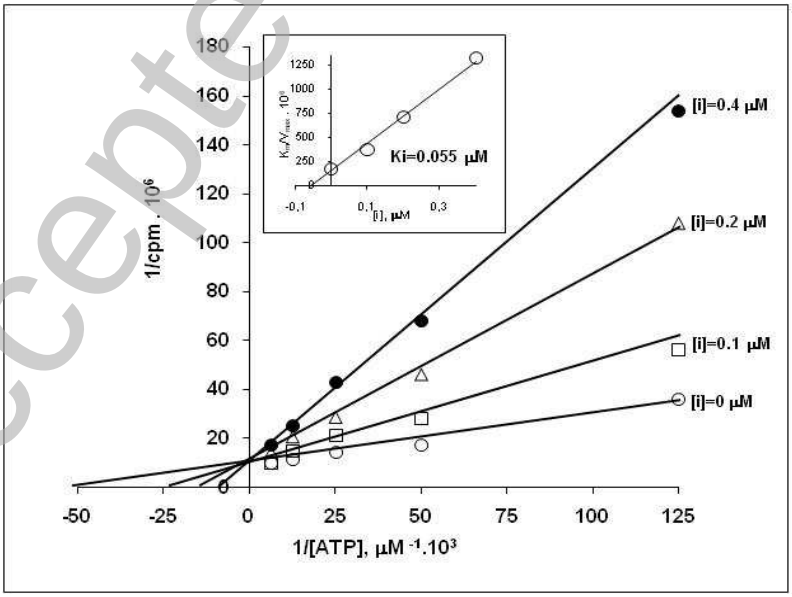

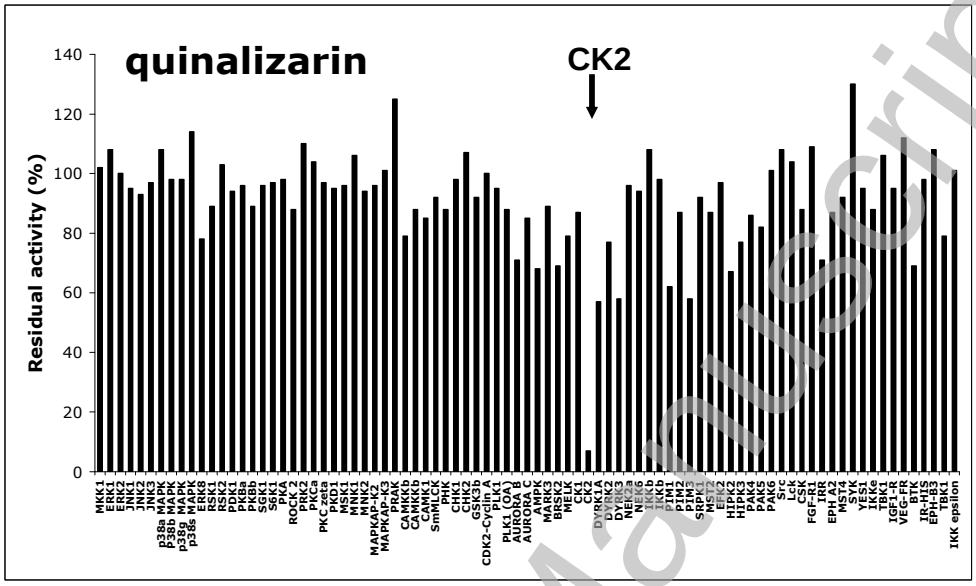

PS = 11.1

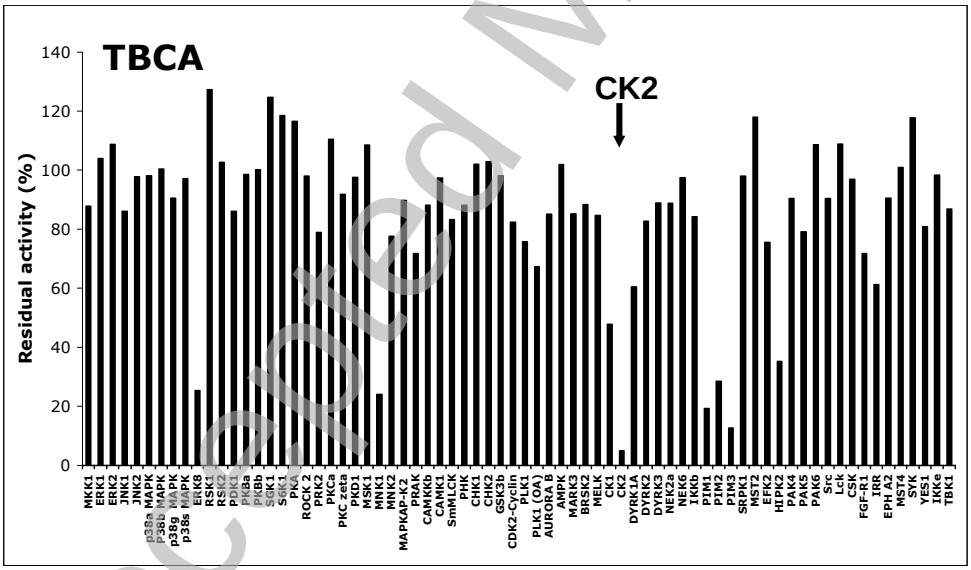

PS = 15.7

Figure 2

Biochemical Journal Immediate Publication. Published on 11 May 2009 as manuscript BJ20090069

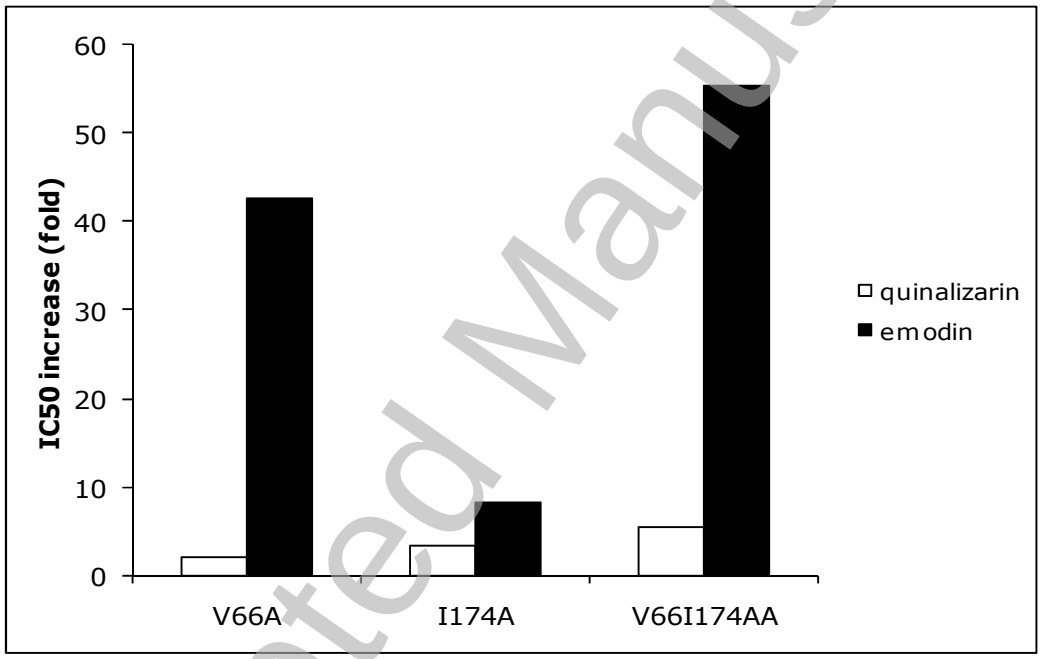

Figure 3

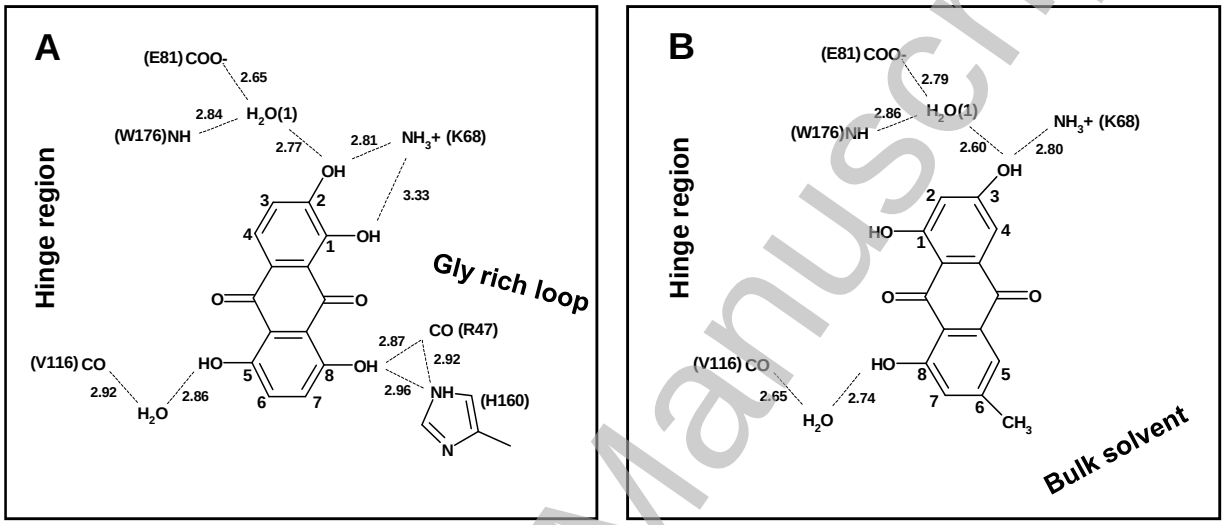

Figure 4

Biochemical Journal Immediate Publication. Published on 11 May 2009 as manuscript BJ20090069

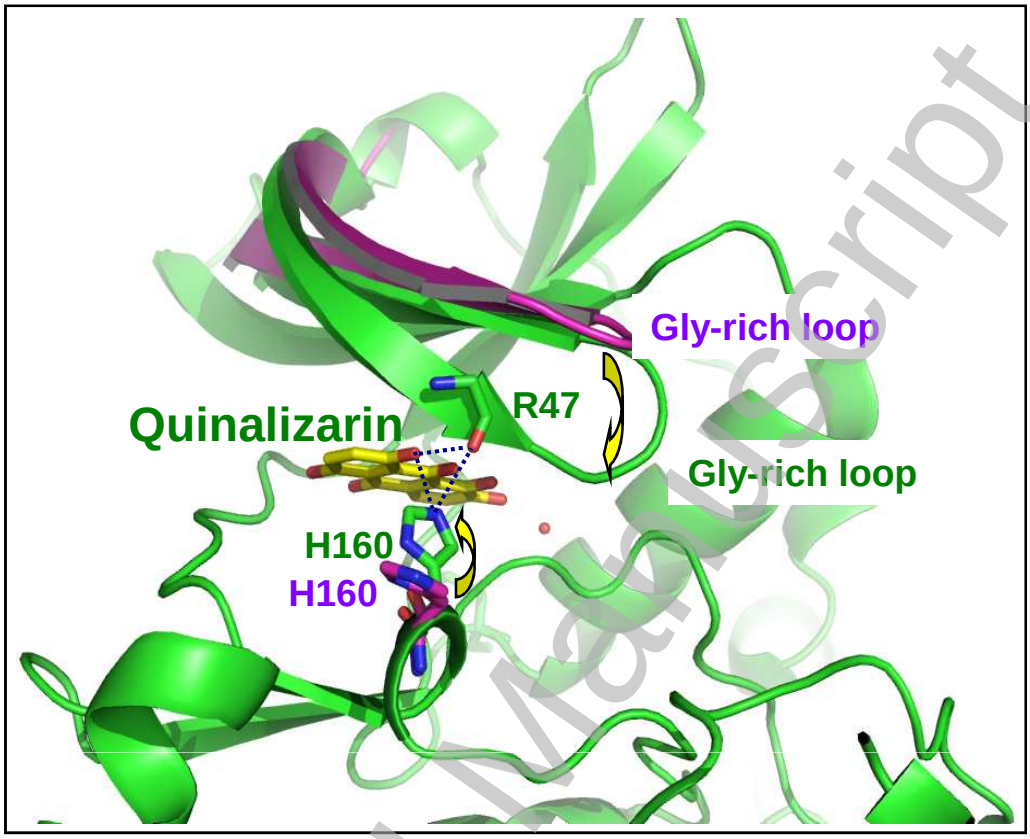

Figure 5

Biochemical Journal Immediate Publication. Published on 11 May 2009 as manuscript BJ20090069

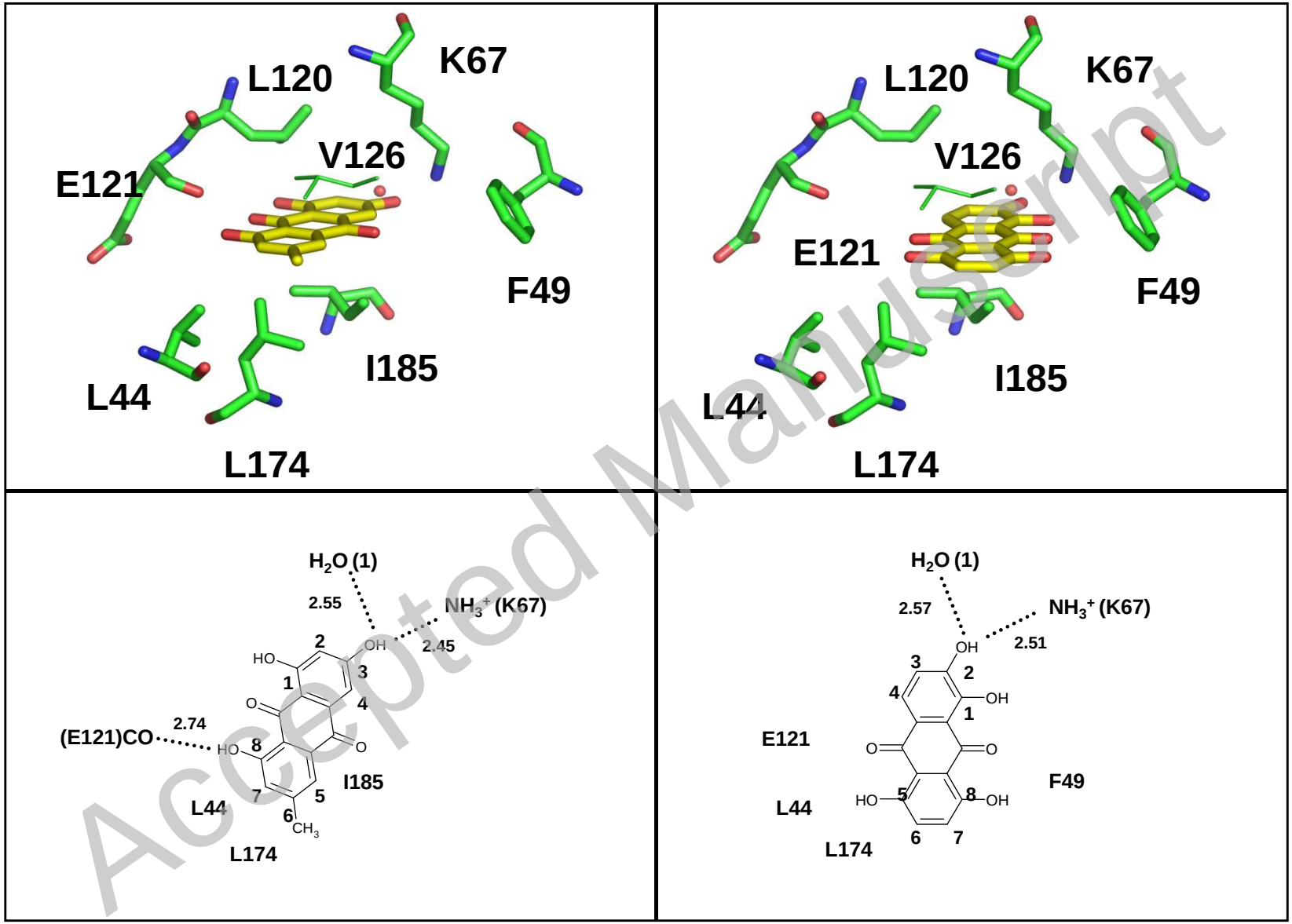

Figure 6

Biochemical Journal Immediate Publication. Published on 11 May 2009 as manuscript BJ20090069

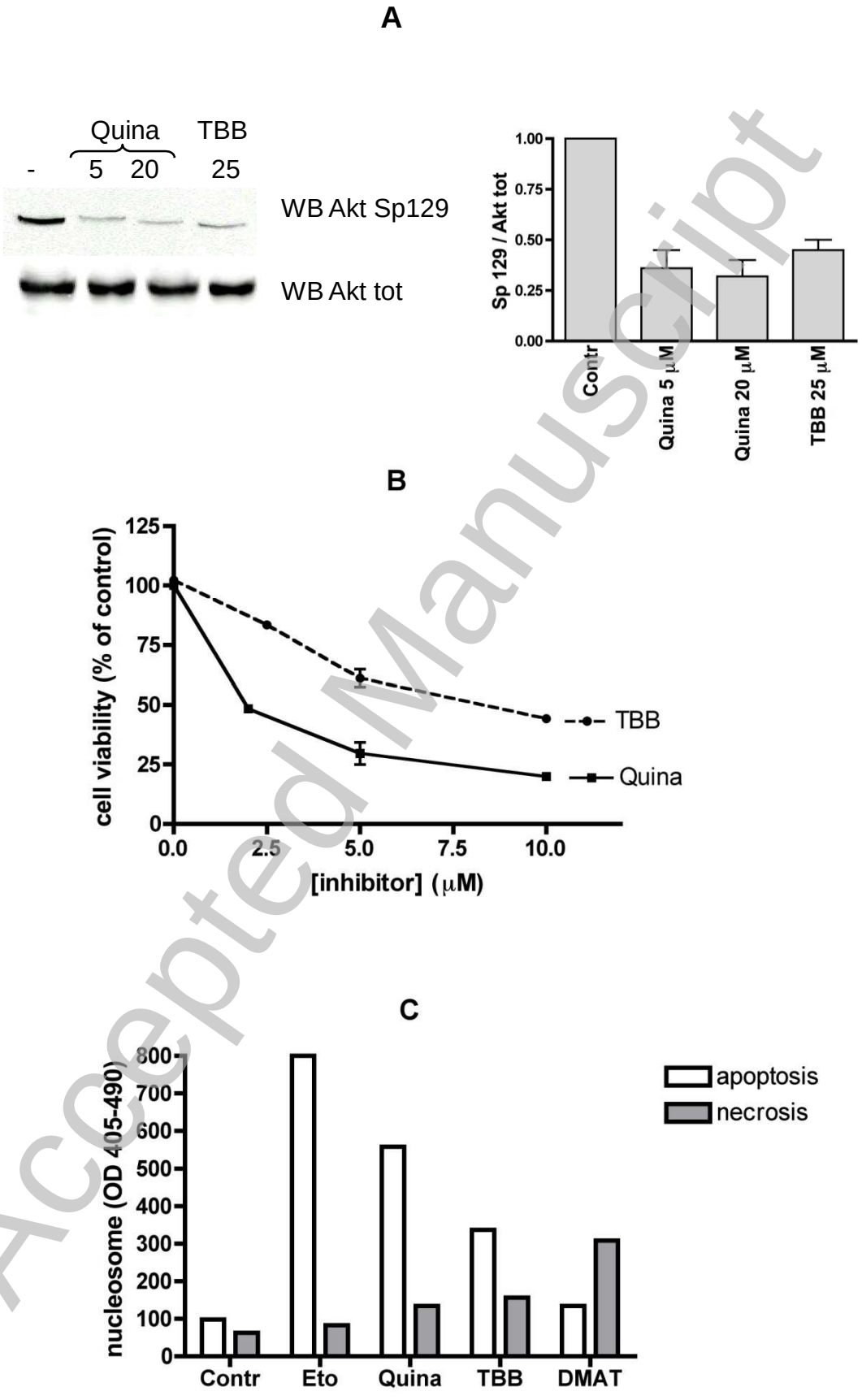

Figure 7